Catal Lett (2011) 141:1703–1708
DOI 10.1007/s10562-011-0699-7

Reductive Amination of Triacetoneamine with *n*-Butylamine Over Cu–Cr–La/γ-Al_2O_3

Meng Sun · Xiaobao Du · Huabang Wang · Zhiwei Wu · Yang Li · Ligong Chen

Received: 13 July 2011 / Accepted: 8 September 2011 / Published online: 21 September 2011

Abstract A series of Cu-based catalysts were prepared and examined for the reductive amination of triacetoneamine with *n*-butylamine, thereinto, Cu–Cr–La/γ-Al_2O_3 showed excellent results. The catalysts were studied by XRD, XPS, H_2-TPR and NH_3-TPD. It was found that doped Cr remarkably enhanced the activity of Cu/γ-Al_2O_3 due to better dispersion of Cu^0, which is believed to be the active site for the reductive amination. Additionally, it was obvious that introduction of La to Cu–Cr/γ-Al_2O_3 led to a higher selectivity and longer lifetime. The reaction parameters were optimized and *N*-butyl-2,2,6,6-tetramethyl-4-piperidinamine was obtained in a yield of 94%.

Keywords Reductive amination · Triacetoneamine · *N*-butylamine · Cu–Cr–La/γ-Al_2O_3

1 Introduction

N-butyl-2,2,6,6-tetramethyl-4-piperidinamine (TEMPBA, b.p. 249.7 °C) obtained by the reductive amination of triacetoneamine (TAA) and *n*-butylamine is a key intermediate of hindered amine light stabilizers (HALS), which have dominated light stabilizers market for several decades due to their excellent light stabilization [1, 2]. It is well known that reductive amination of carbonyl compounds is an important method for the production of amines [3–5]. Up to now, the reductive amination of TAA with *n*-butylamine to TEMPBA in autoclave has been widely described in many studies in the presence of cobalt, nickel, platinum or palladium as catalysts [6, 7]. However, the batch process in autoclave is a tedious process with high energy consumption, environmental pollution and much waste of labor. There are only a few reports concerning about the production of 4-alkylaminopiperidines in a fixed-bed reactor [8, 9], but suffered from expensive catalysts or poor yield. These results encouraged us to develop a continuous process for the production of TEMPBA.

In this work, a continuous process for TEMPBA from triacetoneamine and *n*-butylamine in a fixed-bed reactor over Cu-based catalysts was established. TEMPBA was obtained in 94% yield over Cu–Cr–La/γ-Al_2O_3, which exhibited excellent properties. The effects of Cr and La doped in Cu/γ-Al_2O_3 were studied by XRD, XPS, H_2-TPR and NH_3-TPD.

2 Experimental

2.1 Materials and Catalysts

Triacetoneamine (m.p. 35–39 °C, b.p. 205 °C) was obtained from Beijing Tiangang Auxiliary Co. Ltd, Beijing, China. Commercially available solvents and reagents were used without further purification.

All catalysts used in this study were prepared by coprecipitation-kneading method. For example, $Cu_{20}Cr_5La_5$/γ-Al_2O_3 was prepared as follows. Under mechanical stirring, a mixture of 22.81 g $Cu(NO_3)_2{\cdot}3H_2O$, 11.54 g $Cr(NO_3)_3{\cdot}9H_2O$ and 4.68 g $La(NO_3)_3{\cdot}6H_2O$ in 200 mL H_2O, and a solution of 16.32 g sodium carbonate in 200 mL H_2O were added dropwise into a beaker containing 200 mL H_2O at ambient temperature over 1 h and aged for another 1 h. During the process, the pH of the system was maintained around 8. The precipitate was then filtered,

M. Sun · X. Du · H. Wang · Z. Wu · Y. Li · L. Chen (✉)
School of Chemical Engineering and Technology, Tianjin University, Tianjin 300072, People's Republic of China
e-mail: lgchen@tju.edu.cn

washed with distilled water, dried for 6 h at 110 °C and pulverized. The dried samples were kneaded vigorously with a mixture of 33.07 g pseudo-boehmite and 50 mL 2wt% nitric acid, followed by molding to bars by an extruder. After dried in air for 6 h at 110 °C, the bars were calcined for 4 h at 500 °C and reduced at 220 °C in a hydrogen stream (1.0 MPa) for 4 h before later use.

2.2 Catalysts Characterization

X-ray diffraction (XRD) was carried out on a Rigaka D/max 2500 X-ray diffractometer with Cu-K_α radiation (40 kV, 100 mA) in the range of 5–95°. The mean diameter of Cu crystals was calculated from XRD patterns using Scherrer equation. X-ray photoelectron spectroscopy (XPS) was performed with a PHI 1600 spectroscope using a Mg-K_α X-ray source for excitation. The catalyst samples were removed from the reactor under the protection of nitrogen before XPS analysis. H_2-temperature programmed reduction (H_2-TPR) was measured using a micromeritics 2910 apparatus equipped with a thermal conductivity detector (TCD). The calcined samples were heated from ambient temperature to 600 °C at a rate of 10 °C/min in a mixture of 5% H_2/N_2. NH_3-temperature programmed desorption (NH_3-TPD) was performed with a TP-5000 instrument with a TCD.

2.3 Catalytic Reaction

The catalytic reaction was carried out in a tubular, fixed-bed reactor with an inner diameter of 15 mm and a length of 660 mm, which was loaded with 40.0 mL catalysts. The temperature in the catalyst zone was measured using a thermocouple located in the center of the tube and was regulated by a PID cascade controller. A solution of TAA and *n*-butylamine (molar ratio of 1:1) in 1,4-dioxane (concentration: 14.7%) was stirred for 10 h at ambient temperature, and then dosed into the reactor at a flow rate of 0.3 mL/min by a syringe pump. The GC-MS (Polaris Q, Thermo Finngan, America) used to confirm the components of the reaction mixture was performed on a HP-5 capillary column (30 m × 0.25 mm, 0.2 μm film thickness) equipped with an ion trap MS detector. The composition of the reaction mixture was determined by GC with a 30 m SE-54 capillary column.

3 Results and Discussion

3.1 Catalyst Selection

For reductive amination, hydrogenation/dehydrogenation catalysts such as transition metal based catalysts are often employed. Supported palladium, platinum [9, 10], nickel [11, 12], cobalt [11, 13, 14], copper [15–18] catalysts have been reported to be effective for the reductive amination of ketones or alkanols with alkylamine. Taking the costs of catalysts into consideration, the noble metals were not selected for this reaction. Thus, Ni_{20}/γ-Al_2O_3, Co_{20}/γ-Al_2O_3 and Cu_{20}/γ-Al_2O_3 were prepared and examined for this reaction. The reaction mixture was determined by GC-MS, the main and side reactions occurring during the reductive amination are depicted in Scheme 1. TEMPBA as the main product, 2,2,6,6-tetramethylpiperidin-4-ol

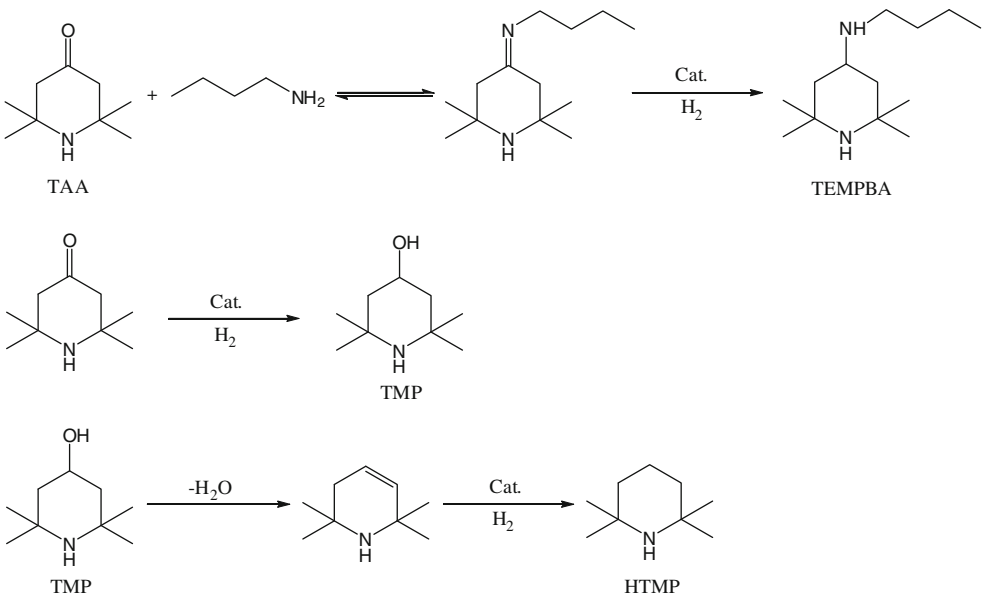

Scheme 1 The reaction process of the reductive amination

Table 1 Results of reductive amination of TAA with *n*-butylamine over various catalysts

Catalyst	TAA conversion (%)	Selectivity (%)		
		HTMP[a]	TMP[b]	TEMPBA[c]
Ni_{20}/γ-Al_2O_3	82.2	3.1	9.7	80.9
Co_{20}/γ-Al_2O_3	87.6	0.5	15.7	70.5
Cu_{20}/γ-Al_2O_3	85.7	3.7	5.1	86.4

Reaction conditions: temperature = 120 °C, hydrogen pressure = 4.0 MPa, flow rate of the solution of TAA and *n*-butylamine = 0.3 mL/min, TAA: *n*-butylamine (mole) = 1:1, concentration of solution = 14.7%

[a] HTMP, 2,2,6,6-tetramethylpiperidine

[b] TMP, 2,2,6,6-tetramethylpiperidin-4-ol

[c] TEMPBA, *N*-butyl-2,2,6,6-tetramethyl-4-piperidinamine

(TMP) and 2,2,6,6-tetramethylpiperidine (HTMP) were detected. TMP was considered to be generated from the direct hydrogenation of TAA, and HTMP would be afforded by the dehydration-hydrogenation of TMP.

The results of the reductive amination of triacetoneamine with *n*-butylamine are summarized in Table 1. All catalysts exhibited satisfied conversion of TAA, but it is obvious that Cu_{20}/γ-Al_2O_3 displayed much better selectivity to TEMPBA than both Ni_{20}/γ-Al_2O_3 and Co_{20}/γ-Al_2O_3. Therefore, copper was chosen as the main catalyst. However, the catalytic activity of Cu_{20}/γ-Al_2O_3 decreased quickly with time-on-stream, the conversion of TAA decreased from 85.7% to 45.3% in 20 h. The color of reaction mixture also turned into greenish from light yellow. The mixture was detected by atomic absorption spectroscopy and Cu was checked out. So, we suggest that the lost of copper may be one reason for the deactivation. What's more, Shiau and Lee [19] reported that the sintering of copper could cause the deactivation of Cu/γ-Al_2O_3. The used Cu_{20}/γ-Al_2O_3 catalyst was characterized by XRD (Fig. 2b) and the mean diameter of Cu^0 particle calculated by Scherrer equation was 875 ± 11 Å, which is much larger than 412 ± 9 Å in the fresh one (Fig. 2c). Thus, it can be deduced that the lost of copper together with the sintering of copper led to the deactivation of Cu_{20}/γ-Al_2O_3.

In order to improve its stability and increase the activity and selectivity, Cr was introduced into Cu_{20}/γ-Al_2O_3 as auxiliary catalyst, and Fe, Mn, La, Zn were doped in Cu-Cr/γ-Al_2O_3 as the third component. The obtained catalysts were then applied to the reductive amination of triacetoneamine with *n*-butylamine, and the results are summarized in Table 2.

As expected, the addition of Cr into Cu_{20}/γ-Al_2O_3 gives rise to an increase in the conversion of TAA. However, the selectivity of TEMPBA was not enhanced obviously. The Cu–Cr/γ-Al_2O_3 doped Fe, Mn, La, Zn showed different results. Thereinto, Cu–Cr-La/γ-Al_2O_3 exhibited the best

Table 2 Results of reductive amination of TAA with *n*-butylamine over the prepared catalysts

Catalyst	TAA conversion (%)	Selectivity (%)		
		HTMP	TMP	TEMPBA
Cu_{20}/γ-Al_2O_3	85.7	3.7	5.1	86.4
$Cu_{20}Cr_5/\gamma$-Al_2O_3	96.4	1.9	3.7	89.7
$Cu_{20}Cr_5Fe_5/\gamma$-Al_2O_3	99.7	2.1	3.0	92.5
$Cu_{20}Cr_5Mn_5/\gamma$-Al_2O_3	99.8	0	7.5	91.8
$Cu_{20}Cr_5La_5/\gamma$-Al_2O_3	99.7	0	2.3	94.5
$Cu_{20}Cr_5Zn_5/\gamma$-Al_2O_3	99.9	1.2	12.6	85.6

Reaction conditions: temperature = 120 °C, hydrogen pressure = 4.0 MPa, flow rate of the solution of TAA and *n*-butylamine = 0.3 mL/min, TAA: *n*-butylamine (mole) = 1:1, concentration of solution = 14.7%

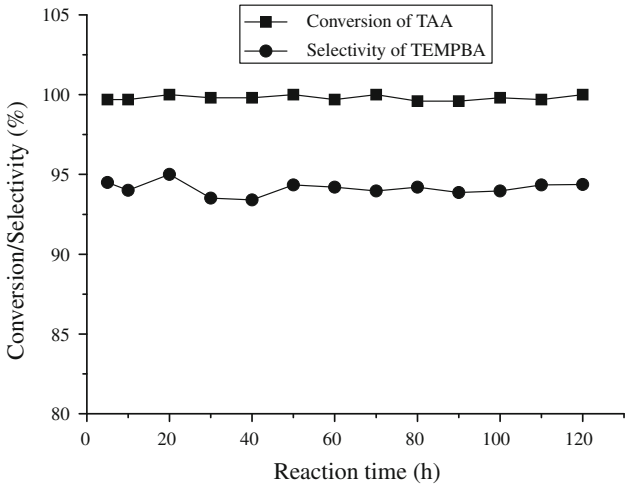

Fig. 1 Service life of $Cu_{20}Cr_5La_5/\gamma$-Al_2O_3

results, especially in the selectivity of TEMPBA, which imply that the doped La can improve the catalytic selectivity remarkably.

3.2 Lifetime of Catalyst

The reaction parameters, including the reaction temperature and the hydrogen pressure, were optimized. Then the catalytic process was performed under optimum reaction conditions for 120 h and the results are shown in Fig. 1. During this period, the catalyst exhibited excellent stability. The conversion of TAA and selectivity of TEMPBA remained around 99.7 and 94.5%, respectively. Therefore, the catalyst could be economically used in large-scale production. XRD, XPS, H_2-TPR and NH_3-TPD were used to characterize these catalysts for further understanding of the results.

3.3 Characterization of Catalysts

3.3.1 XRD

The XRD curves for the unreduced $Cu_{20}Cr_5La_5/\gamma\text{-}Al_2O_3$, reduced $Cu_{20}/\gamma\text{-}Al_2O_3$, reduced $Cu_{20}Cr_5/\gamma\text{-}Al_2O_3$ and reduced $Cu_{20}Cr_5La_5/\gamma\text{-}Al_2O_3$ are shown in Fig. 2. The diffraction lines labeled with "+" in the XRD curve of (a) demonstrate that Cu presents as CuO in the unreduced $Cu_{20}Cr_5La_5/\gamma\text{-}Al_2O_3$. The typical diffraction lines at 43.3°, 50.4°, 74.2° and 90.0° in the XRD curves of (b), (c), (d) and (e) could be assigned to the crystals of elementary copper. It can be found that the addition of Cr and La made Cu crystals smaller and dispersed better. Calculation from the main diffraction line (43.3°) on the XRD patterns using Scherrer equation, the mean diameter of Cu^0 particle decreases from 412 ± 9 Å in the reduced $Cu_{20}/\gamma\text{-}Al_2O_3$ to 211 ± 6 Å and 194 ± 6 Å in the reduced $Cu_{20}Cr_5/\gamma\text{-}Al_2O_3$ and reduced $Cu_{20}Cr_5La_5/\gamma\text{-}Al_2O_3$, respectively. The introduction of Cr led to better dispersion of active species, which can supply more active centers and prevent the sintering of copper. The doped La to $Cu_{20}Cr_5/\gamma\text{-}Al_2O_3$ made this action further enhanced. The more active centers may be the reason for the higher activity of $Cu_{20}Cr_5/\gamma\text{-}Al_2O_3$ and $Cu_{20}Cr_5La_5/\gamma\text{-}Al_2O_3$ compared with $Cu_{20}/\gamma\text{-}Al_2O_3$, which showed in Table 2. No obvious peaks corresponding to Cr, La or any their combinations were picked out from the XRD curves, but it is noticeable that the doped La made the selectivity of TEMPBA enhanced very obviously. We suggest that these components are either too small to be detected or in the amorphous phases.

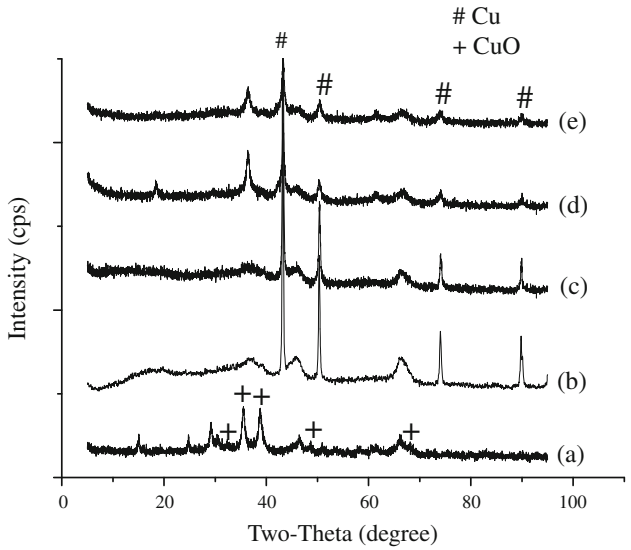

Fig. 2 XRD curves for (*a*) unreduced $Cu_{20}Cr_5La_5/\gamma\text{-}Al_2O_3$, (*b*) used $Cu_{20}/\gamma\text{-}Al_2O_3$, (*c*) reduced $Cu_{20}/\gamma\text{-}Al_2O_3$, (*d*) reduced $Cu_{20}Cr_5/\gamma\text{-}Al_2O_3$ and (*e*) reduced $Cu_{20}Cr_5La_5/\gamma\text{-}Al_2O_3$

3.3.2 XPS

The XPS spectrum of reduced $Cu_{20}Cr_5La_5/\gamma\text{-}Al_2O_3$ is shown in Fig. 3. The peak at 931.99 eV, the binding energy of the Cu 2P3/2 level (Fig. 3a), indicates that Cu exists in

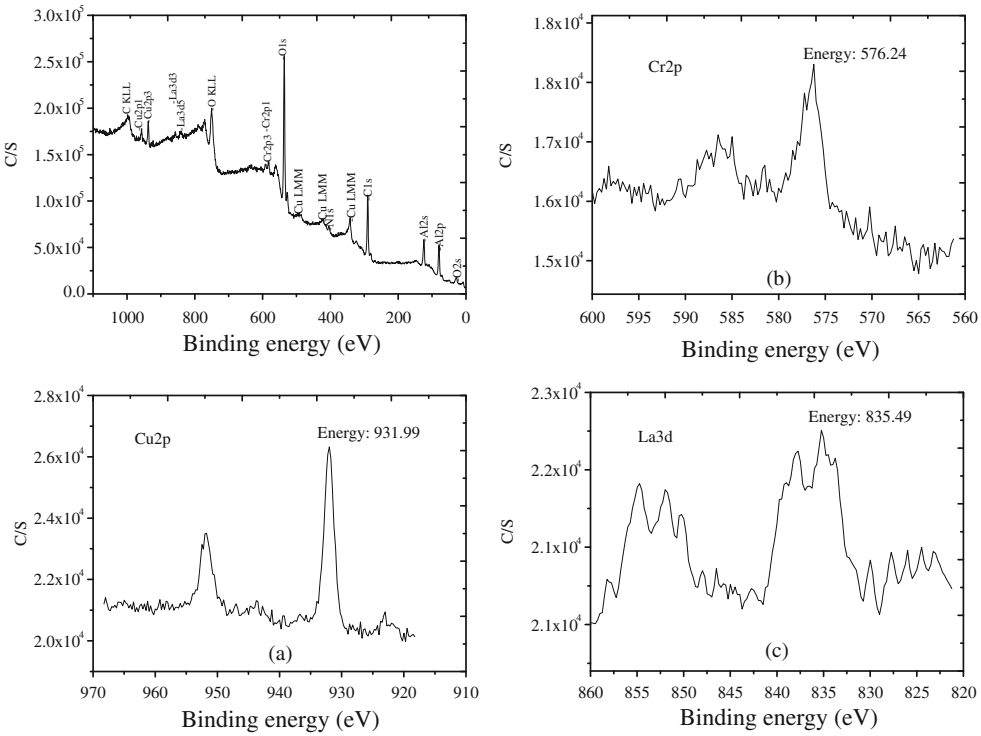

Fig. 3 XPS spectra of the reduced $Cu_{20}Cr_5La_5/\gamma\text{-}Al_2O_3$

$Cu_{20}Cr_5La_5/\gamma\text{-}Al_2O_3$ mainly as Cu^0 species. This assumption could be supported by the typical diffraction lines of the elementary copper crystals in the XRD pattern of the reduced $Cu_{20}Cr_5La_5/\gamma\text{-}Al_2O_3$. The binding energy of the Cr 2p3/2 level (Fig. 3b) at 576.24 eV could be assigned to Cr^{3+}2p3/2. Cr^{3+} may exist as Cr_2O_3 or $CuCr_2O_4$, which could not be identified by our XRD patterns. The binding energy for the La 3d5/2 level at 835.49 eV originates from La^{3+} is probably present as La_2O_3 or $LaAlO_3$, which also could not be identified by XRD patterns.

3.3.3 H_2-TPR

The reducibility of copper species in the calcined catalysts was investigated by H_2-TPR experiments and the results are described in Fig. 4. The unreduced $Cu_{20}/\gamma\text{-}Al_2O_3$ curve displays two signals. The one at T_{max} of 292 °C is corresponding to the typical bulk-like CuO reduction peak, another at T_{max} of 733 °C presumably due to the reduction of aluminate $CuAl_2O_4$ which is much more difficult to reduce [19–22]. For the unreduced $Cu_{20}Cr_5/\gamma\text{-}Al_2O_3$, the reduction temperature of main peak obviously shifts to 234 °C from 292 °C, and the higher temperature peak at 733 °C is disappeared. The peak at 234 °C can probably be attributed to the reduction of highly-dispersed copper oxide, which could be reduced completely at the relatively low temperature [23, 24]. The disappearance of the peak at 733 °C suggests that the addition of chromium can significantly inhibit the formation of aluminate. These results indicate that the chromium addition can not only improve the dispersion of Cu particles but can also prevent copper from reacting with aluminum support to form aluminate. As for the unreduced $Cu_{20}Cr_5La_5/\gamma\text{-}Al_2O_3$, a slight shift of the main reduction peak towards lower temperature (223 °C) compared with that of the unreduced $Cu_{20}Cr_5/\gamma\text{-}Al_2O_3$ and a shoulder peak were detected. We suggest that the existence of La may further improve the dispersion of Cu particles and therefore promote the reducibility of the catalyst. That is why Cu–Cr–La/$\gamma\text{-}Al_2O_3$ showed the best reaction results at the same reduction temperature. These results agree well with the XRD results, and also prove that the reduction temperature at 220 °C is suitable. It should be noted that a new broad peak was also observed at 648–796 °C, this can probably ascribed to the combination of La with the aluminum support. This combination was claimed to inhibit the sintering of high surface area of $\gamma\text{-}Al_2O_3$ [25], which is one of the reasons for the long lifetime of $Cu_{20}Cr_5La_5/\gamma\text{-}Al_2O_3$.

3.3.4 NH_3-TPD

In this present investigation, NH_3-TPD is used to measure the strength of acidity and distribution of acidic sites of the catalysts. The TPD curves of reduced $Cu_{20}/\gamma\text{-}Al_2O_3$, reduced $Cu_{20}Cr_5/\gamma\text{-}Al_2O_3$ and reduced $Cu_{20}Cr_5La_5/\gamma\text{-}Al_2O_3$ are shown in Fig. 5. All the reduced catalysts exhibit a typical double-peak. The two desorption peaks at the lower temperature (229 °C) and the higher temperature (470–529 °C) correspond to the weak and strong acid sites on the catalyst surfaces, respectively [26]. Normally, the area of a specific peak can be used to estimate the amount of ammonia desorbed from the sample, and can be taken as a standard to quantify the acidity of the sample [27, 28]. The peak areas for the two temperature peaks are listed in Table 3. It can be

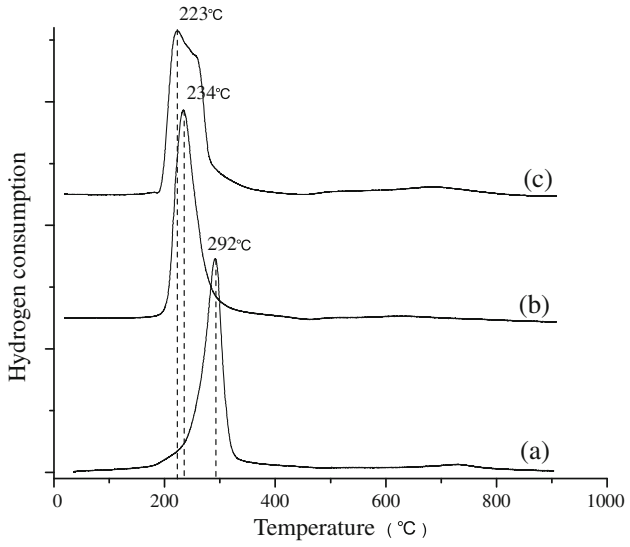

Fig. 4 H_2-TPR curves for (*a*) unreduced $Cu_{20}/\gamma\text{-}Al_2O_3$, (*b*) unreduced $Cu_{20}Cr_5/\gamma\text{-}Al_2O_3$ and (*c*) unreduced $Cu_{20}Cr_5La_5/\gamma\text{-}Al_2O_3$. Operating conditions: 10 °C/min, 5% H_2 in N_2, with total flow rate of 20 mL/min

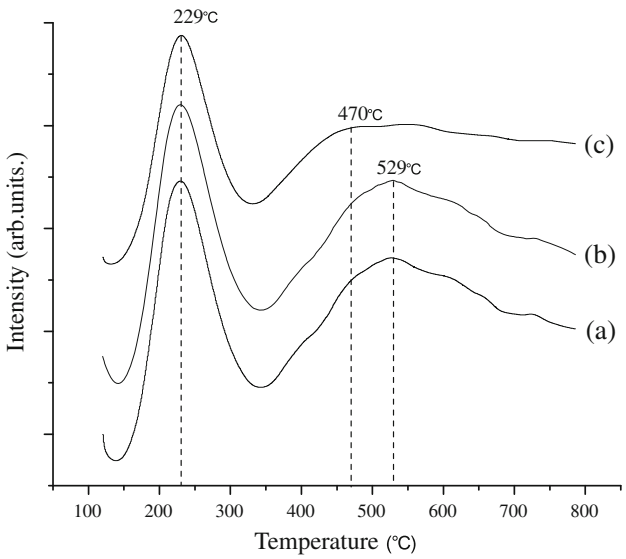

Fig. 5 NH_3-TPD curves for (*a*) reduced $Cu_{20}/\gamma\text{-}Al_2O_3$, (*b*) reduced $Cu_{20}Cr_5/\gamma\text{-}Al_2O_3$ and (*c*) reduced $Cu_{20}Cr_5La_5/\gamma\text{-}Al_2O_3$

Table 3 Temperature programmed desorption of NH_3 for various catalysts

Catalyst	T^a_{des} (°C)	Peak area[c] (a.u.)	T^b_{des} (°C)	Peak area[c] (a.u.)	Total peak area[c] (a.u.)
Cu_{20}/γ-Al_2O_3	229	4161	529	4329	8490
$Cu_{20}Cr_5/\gamma$-Al_2O_3	229	4052	529	4320	8372
$Cu_{20}Cr_5La_5/\gamma$-Al_2O_3	229	3095	470	2404	5499

[a] Lower temperature peak for weak acid sites

[b] Higher temperature peak for strong acid sites

[c] The peak area was calculated by Gaussian fitting method

concluded that the addition of Cr does not impact obviously on the total acidity of Cu_{20}/γ-Al_2O_3. However, with the addition of La to Cu–Cr/γ-Al_2O_3, the areas of desorption peaks decrease remarkably and the higher temperature peak shifts from 529 to 470 °C. This may be caused by the basicity of La_2O_3.

The NH_3-TPD results indicate that the La addition not only decreases the total acidity but also reduces the strength of acid sites. Chary et al. [15] reported in their study that the strong acidic sites are responsible for cyclohexanol dehydration activity. In this work, the dehydration of TMP was inhibited due to the decrease of the acid sites, and that is why the selectivity of TEMPBA was enhanced by the addition of La. It was also reported that strong acid sites facilitate the adsorption of amino compounds on the surface of catalyst and ultimately led to deactivation of the catalyst [29]. The decrease of strong acid sites could be another reason for the long lifetime of $Cu_{20}Cr_5La_5/\gamma$-Al_2O_3.

4 Conclusion

A continuous process for the preparation of *N*-butyl-2,2,6,6-tetramethyl-4-piperidinamine over $Cu_{20}Cr_5La_5/\gamma$-Al_2O_3 in a fixed-bed reactor was established in this work. Cu^0 is believed to be the active species for the reductive amination of triacetoneamine with *n*-butylamine. The doped Cr can not only improve the dispersion of copper particles but can also prevent copper from reacting with aluminum support to form aluminate. The introduction of La was found to result in a higher selectivity and longer lifetime. *N*-butyl-2,2,6,6-tetramethyl-4-piperidinamine was obtained in 94% yield over $Cu_{20}Cr_5La_5/\gamma$-Al_2O_3 and this process could be applicable for large-scale industrial production.

Acknowledgment The authors would like to express their thanks for the financial support provided by the National Natural Science Foundation of China (Grant No. 20976123).

References

1. Kai-Uwe S (2010) WO2010142572
2. Jochen K, Peter W, Guenter K, Edeltraud K (2007) WO2007057265
3. Devi CL, Olusegun OS, Kumar CNSSP, Rao VJ, Palaniappan S (2009) Catal Lett 132:480
4. Prakash GKS, Do C, Mathew T, Olah GA (2010) Catal Lett 137:111
5. Kirumakki SR, Papadaki M, Chary KVR, Nagaraju N (2010) J Mol Cat A Chem 321:15
6. Malz Jr. RE, Greefield H (1986) US4607104
7. Wiezer H (1981) DE3007996
8. Disteldorf DJ, Zur Hausen DM, Hubel DW, Kriebel DG (1984) EP0128285
9. Jegelka U, Kreilkamp G (1999) US5945536
10. Gomez S, Peters JA, van der Waal JC, Maschmeyer T (2003) Appl Catal A 254:77
11. Sewell G, O'Connor C, van Steen E (1995) Appl Catal A 125:99
12. Zamlynny V, Kubelkova L, Baburek E, Jiratova K, Novakova J (1998) Appl Catal A 169:119
13. Sewell GS, O'Connor CT, van Steen E (1997) J Catal 167:513
14. Zhang Y, Zhang YC, Feng C, Qiu CJ, Wen YL, Zhao JQ (2009) Catal Commun 10:1454
15. Chary KVR, Seela KK, Naresh D, Ramakanth P (2008) Catal Commun 9:75
16. Dume C, Holderich WF (1999) Appl Catal A 183:167
17. Yamakawa T, Tsuchiya I, Mitsuzuka D, Ogawa T (2004) Catal Commun 5:291
18. Mahdavi V, Peyrovi MH (2006) Catal Commun 7:542
19. Shiau CY, Lee YR (2001) Appl Catal A 220:173
20. Dow WP, Wang YP, Huang TJ (1996) J Catal 160:155
21. Bridier B, López N, Pérez-Ramírez J (2010) J Catal 269:80
22. Ferrandon M, Bjornbom E (2001) J Catal 200:148
23. Van der Grift CJG, Mulder A, Geus JW (1990) Appl Catal 60:181
24. Roberstson SD, McNicol BD, de Baas JH, Kloet SC, Jenkins JW (1975) J Catal 37:424
25. Church JS, Cant NW, Trimm DL (1993) Appl Catal A 101:105
26. Wang CH, Weng HS (1998) Appl Catal A 170:73
27. Meshram NR, Hegde SG, Kulkarni SB (1986) Zeolites 6:434
28. Ma D, Zhang WP, Shu YY, Liu XM, Xu YD, Bao XH (2000) Catal Lett 66:155
29. Bartholomew CH (2001) Appl Catal A 212:17